Dynamics of the H + O_2 → O + OH Chain-Branching Reaction: Accurate Quantum Mechanical and Experimental Absolute Reaction Cross Sections

Mohammed Abu Bajeh,[†] Evelyn M. Goldfield,[‡] Alexander Hanf,[†] Christoph Kappel,[§] Anthony J. H. M. Meijer,*[,||] Hans-Robert Volpp,[†] and Jürgen Wolfrum[†]

Physikalisch-Chemisches Institut, Universität Heidelberg, Im Neuenheimer Feld 253, D-69120 Heidelberg, Germany, Department of Chemistry, Wayne State University, Detroit, Michigan 48202, Institut für Physikalische Chemie der Universität Göttingen, D-37075 Göttingen, Germany, and Department of Chemistry, University College London, London WC1H 0AJ, United Kingdom

Received: October 4, 2000; In Final Form: December 15, 2000

The H + O_2 → O + OH chain-branching reaction, one of the most important elementary reactions in combustion chemistry, represents a challenging benchmark system for testing dynamical theories against experiments. The translational energy dependence of the total reaction cross section of the H + O_2 (vibrational quantum number $v = 0$) reaction was investigated experimentally employing a pulsed laser pump−probe technique and theoretically by means of quantum mechanical scattering calculations. The present results indicate that there is no sharp increase in reactivity for translational energies $E_{tr} \geq 1.4$ eV as was suggested by earlier experiments and approximate dynamical calculations. Furthermore, our results indicate that the potential energy surface needs to be improved to achieve quantitative agreement between experiment and theory.

Introduction

The development of laser-based "pump−probe" techniques which combine pulsed laser photolysis to generate energy state-selected reagents with time- and quantum state-resolved laser spectroscopic reaction product detection[1] along with the progress made in the quantum mechanical treatment of reactive scattering processes[2] has paved the way for detailed studies of the molecular dynamics of elementary gas-phase reactions.[3] However, in contrast to the benchmark atom−molecule reaction H + H_2 → H_2 + H for which impressive quantitative agreement between experiment and theory has been achieved in recent years,[4−7] key features of the microscopic dynamics of the simplest gas-phase reaction of molecular oxygen

$$H + O_2(\tilde{X}\ ^3\Sigma_g^-) \rightarrow O(^3P) + OH(^2\Pi) \qquad (1)$$

which represents one of the most important elementary reaction in combustion chemistry[8,9] are still not resolved.

An unresolved feature for this reaction is the sharp maximum in the total reaction cross section $\sigma_R(E_{tr})$ for the H + $O_2(v = 0)$ reaction located at a reactant translational energy E_{tr} of approximately 1.8 eV,[10,11] which was observed in reaction dynamics studies employing translational energy-selected H atoms in combination with laser spectroscopic quantum-state-resolved OH($^2\Pi$) reaction product detection.[12−14] This remarkable finding initiated a number of theoretical studies comprising statistical calculations based on transition state theory (TST) as well as of quasiclassical trajectory (QCT) calculations.[8,10,15] Although these calculations were not successful in reproducing the experimental reaction cross section, important conclusions about the reaction mechanism were drawn[16−18] from these studies, while at the same time inherent limitations of the TST and QCT approaches became obvious.[15] Detailed analysis of the QCT calculations indicated the presence of a large number of trajectory recrossings of transition state dividing surfaces (in violation of transition state theory) and further revealed that many reactive trajectories lead to the formation of OH products with less than the quantum mechanical vibrational zero-point energy.[15] Although in a number of subsequent QCT calculations various a posteriori correction schemes were applied to account (in an approximate way) for the intrinsic inability of classical mechanics to conserve zero-point energy, no satisfactory agreement between the experimental and theoretical reaction cross sections was obtained. (More sophisticated "active" methods which control the flow of zero-point energy during the course of individual trajectories have been discussed[19] but have not yet been applied to the H + O_2 reaction.) It was concluded that further reaction cross section measurements along with rigorous quantum mechanical calculations were required to resolve the discrepancy between theory and experiment.[8] In general, such rigorous quantum mechanical calculations can serve as a test for the employed potential energy surface (PES) as well as for more approximate methods, e.g. based on classical mechanics[20] or advanced statistical rate theories such as the statistical adiabatic channel model (SACM).[21,22] However, converged quantum mechanical calculations are notoriously difficult and computationally expensive. Thus, only a handful of atom−diatom gas-phase reactions have been treated rigorously using quantum mechanics so far, such as e.g., H + H_2/D_2[23,24] and F + H_2.[25]

Accurate Quantum Mechanical Scattering Calculations

There are three particular features associated with reaction 1 which make accurate quantum mechanical scattering calculations for this reaction challenging. First, the ground-state PES has a deep well (see Figure 1A,B), corresponding to the stable

* Corresponding author: E-mail a.meijer@ucl.ac.uk. Fax: +44-(0)20-7679-7463.
[†] Universität Heidelberg.
[‡] Wayne State University.
[§] Institut für Physikalische Chemie der Universität Göttingen.
[||] University College London.

10.1021/jp0036137 CCC: $20.00
Published on Web 02/24/2001

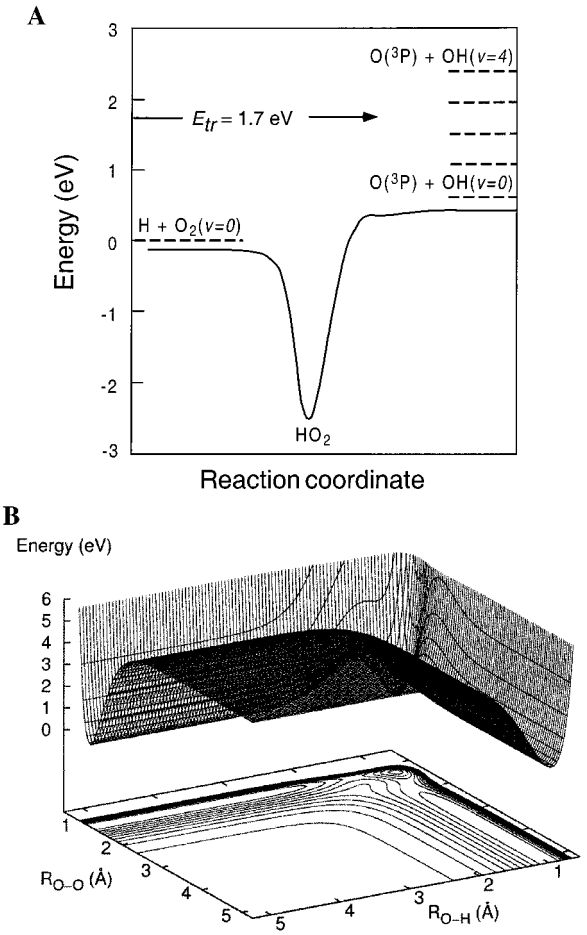

Figure 1. (A) Energy level diagram for the $H + O_2 \rightarrow O + OH$ reaction together with a schematic representation of the minimum energy path on the DMBE IV potential energy surface (shown as a solid curve). Energies are given with respect to the vibrational zero-point energy of the $H + O_2$ reagents. The maximum reagent translational energy ($E_{tr} = 1.7$ eV) considered in the quantum mechanical reaction cross section calculations is indicated with an arrow. (B) Contour map and three-dimensional representation of the DMBE IV potential energy surface for a collinear collision geometry. R_{O-H} denotes the distance between the hydrogen atom and the "middle" oxygen atom. R_{O-O} denotes the distance between the two oxygen atoms.

hydroperoxyl radical $HO_2(\tilde{X}^2A'')$, which supports many bound states and resonances. Second, the PES in the $O(^3P) + OH(^2\Pi)$ product arrangement channel is governed by a long-range dipole-induced quadrupole interaction potential which is longer ranged ($\propto R^{-4}$, with R being the distance between the O atom and the center-of-mass of the OH radical) than the usual van der Waals ($\propto R^{-6}$) interaction. Third, there are two "heavy" (i.e. non-hydrogen) atoms involved in this reaction. Hence, large grids and consequently large propagation times (in case of an iterative method) are needed to converge the calculations. As a consequence, quantum mechanical calculations for this reaction have become possible only recently. Most of these calculations were performed for total angular moment $J = 0$ (nonrotating HO_2 system) only[26,27] or were based on results obtained for $J = 0$ in combination with the J-shifting approximation to account for $J > 0$ contributions.[28] Unlike in the case of reactions with a barrier, however, the J-shifting approximation was found to be of questionable validity in case of reaction 1 emphasizing the need for rigorous calculations for $J > 0$.[27] Such rigorous coupled channel (CC) calculations on the double many-body expansion (DMBE IV) potential energy surface (PES) of Varandas and co-workers[29] were recently performed.[30] The results presented in the following represent an extension of these studies toward the calculation of total reaction cross sections on the basis of the accurate $J > 0$ total reaction probabilities in the translational energy range $E_{tr} \leq 1.7$ eV.

To calculate total reaction cross sections $\sigma_R^{(v,j)}$ out of an given initial O_2 rovibrational state (v, j) as a function of the reagent translational energy (E_{tr}), in the present study the following relation is used

$$\sigma_R^{(v,j)}(E_{tr}) = \frac{1}{g}\frac{\pi}{k_{vj}^2}\frac{1}{(2j+1)}\sum_{JK_0p}(2J+1)P_{JK_0p}^{(v,j)}(E_{tr}) \qquad (2)$$

where k_{vj} is the wavenumber associated with the translational energy E_{tr} ($k_{vj} = \sqrt{2\mu E_{tr}}$) with μ being the reduced mass of the $H + O_2$ reagent collision pair. $P_{JK_0p}^{(v,j)}(E_{tr})$ is the reaction probability out of the initial state $O_2(v, j)$ reagent state for a given total angular momentum quantum number J, parity p of the wave function, and initial projection quantum number K_0 of the total angular momentum vector $\bar{\mathbf{J}}$ onto the z-axis of the coordinate system (in this case the vector connecting the H atom with the center-of-mass of the O_2 molecule). In eq 2, the factor of $1/g$ (with $g = 3$) accounts for the electronic degeneracy of the $H(^2S) + O_2(\tilde{X}\ ^3\Sigma_g^-)$ reagent system and represents the probability of a given collision to occur on the ground-state ($^2A''$)-PES which correlates adiabatically with $O(^3P) + OH(^2\Pi)$ products.[31−33]

Besides the factors mentioned above, which are more or less specific to the $H + O_2$ system, there are two additional factors which make the calculation of total reaction cross sections computationally expensive. First, the summation over J in eq 2 can run to large values of J, making a large number of calculations for different values of J necessary. Second, even though J and p are conserved during a calculation, K is most definitely not. This means that for a given value of J there are either $J + 1$ or J substates, labeled by K, which need to be taken into account (note that this number would be $2J + 1$ had we not parity-adapted the wave function). As a result a calculation for e.g. $J = 10$ is approximately 10 times more expensive than a calculation for $J = 0$. However, the Coriolis coupling between states with a different value of K is tridiagonal in nature; i.e., a state with quantum number K only couples to states with quantum number $K + 1$ or $K - 1$. *This fact can be exploited by performing the calculation on a parallel computer, whereby each processor is assigned a part of the wave function with a specific quantum number K.* This "Coriolis coupled method",[29] is highly parallel, meaning that a $J = 10$ calculation on 10 or 11 (depending on parity) processors can be performed in the same time as a $J = 0$ calculation on one processor. This makes $J > 0$ calculations on a system like $H + O_2$ feasible.

In the present work the time-dependent wave packet formalism in combination with the flux method of ref 25 was used to calculate reaction probabilities $P_{JK_0p}^{(0,1)}(E_{tr})$ for the $H + O_2(v = 0, j = 1) \rightarrow OH + O$ reaction. We had to introduce an approximation to calculate the reaction cross sections. It turns out to be unfeasible to calculate $P_{JK_0p}^{(0,1)}(E_{tr})$ for each value of J that contributes to the sum in eq 2. Instead, we have chosen to calculate $P_{JK_0p}^{(0,1)}(E_{tr})$ on a grid of J values. These reaction probabilities were subsequently used to generate the reaction probabilities for other values of J in order to evaluate the sum over J in eq 2. The complete procedure for calculating the cross sections is as follows: First we calculate the reaction probabilities on a grid of J values (in the present case $J = 0$, 1, 2, 5, 10, 15, 20, 25, and 35). These reaction probabilities were subsequently smoothed using a [25,25,2]-Savitzky−Golay

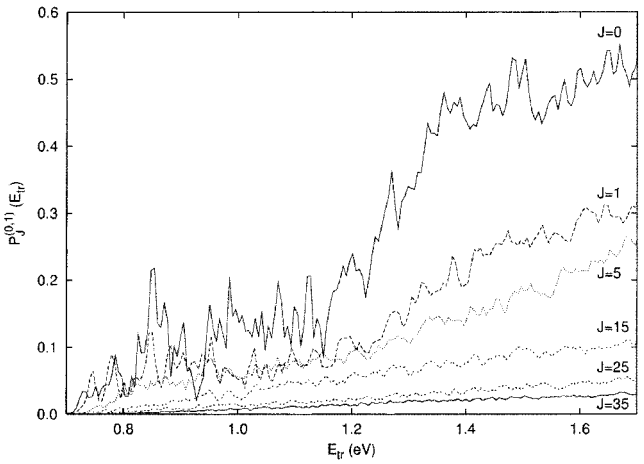

Figure 2. Quantum mechanical reaction probabilities $P_J^{(0,1)}(E_{tr})$ for different values of the total angular momentum J plotted against the H + O_2 reagent translational energy $E_{tr.}$

smoothing filter.[34] This ensures that no unphysical resonances will appear in the cross sections. The smoothed reaction probabilities were fitted at one particular collision energy to a second-order polynomial in J. This fit was performed for a range of collision energies. Subsequently, these fits were used to interpolate the reaction probabilities to get the reaction probabilities at intermediate values of J. We used a simple linear extrapolation for values of J beyond 35. The extrapolation was stopped as soon the reaction probability reached zero. In practice, this meant we extended our calculations up until $J = 65$ for some translational energies. A number of different interpolation/extrapolation algorithms and fitting polynomials were tried but were found to have an insignificant influence on the final result.

Detailed quantum mechanical calculations of state-to-state reaction probabilities revealed that the initial rotational excitation of O_2 has no pronounced effect on reactivity,[26] and QCT calculations further demonstrated that the value of the reaction cross section only varies slightly over the range of $O_2(v = 0, j = 1, 3, ...)$ rovibrational states[35] typically populated at room temperature.[10] Therefore, the reaction cross sections $\sigma_R^{(0,1)}(E_{tr})$ obtained from the $P_{JK_0p}^{(0,1)}(E_{tr})$ reaction probabilities should allow for a meaningful comparison with results of reaction cross section measurements carried out with room-temperature O_2 reagents which will be most likely in the rotational states $j = 7, 9$ of the $O_2(v = 0)$ vibrational ground state.

Before we compare the calculated reaction cross sections with experimental measurements we will briefly discuss the J-dependence of the (unfiltered) total reaction probabilities $P_J^{(0,1)}(E_{tr})$−where $P_J^{(0,1)}(E_{tr})$ is the average of all $P_{JK_0p}^{(0,1)}(E_{tr})$ for a given J−and its consequences on approximate quantum mechanical dynamical treatments. As it can be seen in Figure 2, the $J = 0$ reaction probabilities are much larger than those obtained for $J > 0$. Therefore, reaction cross section calculated using dynamical information from only $J = 0$ calculations will overestimate the "true" reaction cross section (see e.g. refs 36 and 37). A second implication of the pronounced reduction in reaction probability for $J > 0$ as observed in the present calculations is that the maximum value of J actually needed to calculate converged cross sections is much less than would be estimated by an extrapolation method based solely on the $P_{J=0}^{(0,1)}(E_{tr})$ reaction probabilities, since these methods usually assume a smooth decay of the reaction probability as a function of J. Another important effect concerns the appearance of resonance structures in the reaction cross section. An approximate treatment based on $P_{J=0}^{(0,1)}(E_{tr})$ will yield a reaction cross section with a rich resonance structure (closely resembling the resonance features of the $P_{J=0}^{(0,1)}(E_{tr})$ reaction probability),[36] whereas rigorous calculations will result in a much smoother translational energy dependence. The latter is a direct consequence of the summation over the individual reaction probabilities with $J > 0$. For $J > 0$ the resonances in the reaction probabilities become less pronounced, because different K states have their resonances at slightly different translational energies. Correct treatment of the Coriolis coupling is very important in this respect.[29] For a more elaborate discussion of the theoretical results, see ref 38.

Absolute Reaction Cross Section Measurements

Along with the quantum mechanical calculations absolute reaction cross section measurements were performed using the photochemical technique of Kuppermann for the preparation of "fast" H atoms with well-defined translational energies.[39] In the present experiments pulsed laser flash photolysis of H_2S or HBr at an UV wavelength of 222 nm was employed for the generation of translationally excited H atoms.[40] In combination with time-resolved pulsed laser induced fluorescence detection of $O(^3P)$ atom products this experimental approach allows the direct determination of the complete $O(^3P_{j'=2,1,0})$ reaction product fine-structure state population,[41] contrary to earlier gas-phase reaction dynamics studies in which the complementary OH reaction products were probed. As has been demonstrated in refs 42 and 43, total reaction cross section measurements based on O atom detection can be used to eliminate the uncertainties originating from the various extrapolation schemes that had to be applied in earlier measurements in order to estimate the contribution of spectroscopically inaccessible rovibrational OH product states to the total reaction cross section.[44]

The reaction cross section measurements were carried out using the pulsed laser "pump-and-probe" setup described in detail elsewhere.[42,43] It consists of a flow reactor through which sample gas mixtures containing the H atom precursor compounds (H_2S or HBr) together with O_2 at room temperature are slowly flowed with partial pressures of typically 20−40 and 90−150 mTorr, respectively. The reaction is initiated by irradiating the H_2S/O_2 and HBr/O_2 mixtures with a UV "pump" excimer laser pulse (pulse duration ∼15 ns, emission wavelength 222 nm), which selectively photodissociates the H atom precursor molecule. This generates energetic H atoms with average translational energies of $E_{tr} = 1.56$ eV and $E_{tr} = 1.66$ eV, respectively, which subsequently react with O_2 molecules. The $O(^3P_{j'})$ reaction products are detected under single-collision conditions by a subsequent "probe" laser pulse (pulse duration ∼10 ns), delayed with respect to the "pump" laser pulse by typically 120−150 ns. Fine-structure resolved detection of nascent $O(^3P_{j'})$ atoms (see Figure 3A) is achieved by laser induced fluorescence (LIF) excitation of the $O(3s\ ^3S^\circ \leftarrow 2p\ ^3P_{j'})$ spectral transitions at $\lambda_{probe} = 130.22$ nm ($j' = 2$), 130.48 nm ($j' = 1$), and 130.60 nm ($j' = 0$) using tunable vacuum-UV probe laser light. It was found that the VUV probe beam itself produced appreciable $O(^3P_{j'=2,1,0})$ atom LIF signals via the photolysis of O_2 and NO_2, respectively. To subtract these "background" $O(^3P_{j'=2,1,0})$ atoms from the $O(^3P_{j=2,1,0})$ atoms produced in the H + O_2 reaction and in the 222 nm photolysis of NO_2, respectively, an electronically controlled mechanical shutter was inserted into the photolysis beam path. At each point of the O atom spectral line scan, the signal was first averaged with the shutter opened and again averaged with the shutter closed. A point-by-point subtraction procedure was adopted, to

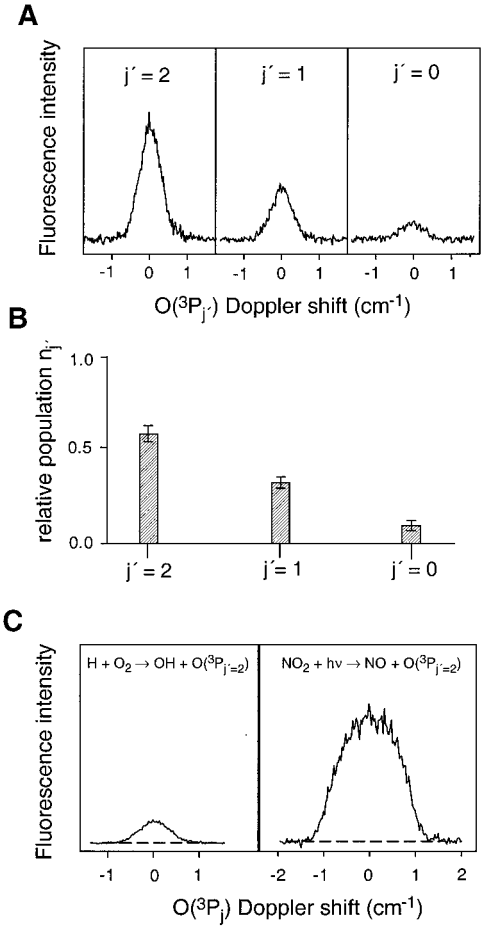

Figure 3. (A) Fluorescence excitation spectra of the three fine-structure states ($j' = 2, 1, 0$) of $O(^3P)$ product atoms formed in the reaction of translational energetic H atoms ($E_{tr} = 1.56$ eV) with room-temperature O_2. The spectra were recorded 120 ns after pulsed UV-laser flash photolysis (222 nm) of 34 mTorr of H_2S in the presence of 149 mTorr of O_2. The measured fluorescence intensity is plotted against the O atom Doppler shift. The centers of the spectra correspond to the (3s $^3S^o \leftarrow$ 2p $^3P_{j'}$)-transitions of the $j' = 2, 1, 0$ fine-structure states of $O(^3P)$ at $\lambda_{probe} = 130.22$, 130.48, and 130.60 nm, respectively. (B) Relative population of the $j' = 2, 1, 0$ fine-structure states of the nascent $O(^3P)$ reaction products derived from the integrated areas of fluorescence excitation spectra shown in (A). (C) Comparison between the fluorescence excitation spectrum of $O(^3P_{j'=2})$ atoms produced in the H + O_2 reaction (experimental conditions as in (A)) and an $O(^3P_{j'=2})$ reference fluorescence excitation spectrum recorded after pulsed UV-laser flash photolysis of 25 mTorr of NO_2 (both spectra are on the same vertical scale). Details about the photolytic calibration method for the determination of absolute reaction cross sections for the H + $O_2(v = 0) \rightarrow$ O + OH reaction are given in refs 40 and 41.

obtain directly and on-line a fluorescence signal free from "probe-laser-generated" background O atoms. In the reaction measurements the background O atom LIF signal was typically about 2% of the background corrected LIF signal, and in the NO_2 dissociation measurements the background signal was about 5% of the background corrected signal. From the background-corrected fluorescence excitation spectra shown in Figure 3A the relative population $n_{j'}$ of the three fine-structure states of the $O(^3P_{j'=2,1,0})$ atom reaction products and hence their relative contribution to the total reaction cross section could be obtained (see e.g. Figure 3B) taking into account the different oscillator strengths of the spectral transitions. As outlined in ref 12 in order to obtain an absolute value for the reaction cross section from LIF measurements an independent calibration of the product detection sensitivity is required. In the present experiments this calibration was performed by comparing the $O(^3P_{j'=2})$ LIF signal intensities obtained in the H + O_2 reaction with the $O(^3P_{j'=2})$ LIF signal intensities of well-defined $O(^3P_{j'=2})$ atom reference concentrations generated via the photodissociation of NO_2, respectively.[39,41] For those measurements in which the UV-photodissociation of H_2S was employed for H atom generation the total absolute reaction cross section σ_R can be by obtained employing the following formula:[40,41]

$$\sigma_R(1.56\text{ eV}) = \gamma \frac{S_R(j'=2) N_{j'=2} \quad \phi_O \sigma_{NO_2}[NO_2]}{S_C(j'=2) n_{j'=2} \sigma_{H_2S}[H_2S][O_2] v_{rel} \Delta t} \quad (3)$$

Here v_{rel} is the relative velocity which corresponds to the average translational energy of $E_{tr} = 1.56$ eV of the H + O_2 reactant pair. $\phi_O = 0.61 \pm 0.07$ stands for the total $O(^3P)$ product quantum yield in the 222 nm photolysis of NO_2 and $\sigma_{H_2S} = (9.3 \pm 0.3) \times 10^{-19}$ cm^2 and $\sigma_{NO_2} = (4.2 \pm 0.2) \times 10^{-19}$ cm^2 are the optical absorption cross sections of H_2S and NO_2 at the pump laser wavelength of 222 nm. In eq 3 [NO_2], [H_2S], and [O_2] denote the respective gas-phase concentrations of NO_2, H_2S, and O_2 and Δt is the time delay between pump and probe laser pulses. $n_{j'=2}$ and $N_{j'=2}$ are the relative populations of the $O(^3P_{j'=2})$ fine-structure state determined in the H + O_2 reaction ($n_{j'=2}/n_{j'=1}/n_{j'=0} = 0.58 \pm 0.03/0.33 \pm 0.02/0.09 \pm 0.01$; see Figure 3B) and in the 222 nm photolysis measurements of NO_2, respectively ($N_{j'=2}/N_{j'=1}/N_{j'=0} = 0.52 \pm 0.03/0.33 \pm 0.01/0.15 \pm 0.02$). $S_R(j'=2)$ and $S_C(j'=2)$ are the integrated LIF signal intensities (obtained from the integrated areas below the respective fluorescence excitation curves depicted in Figure 3C) measured in the H + O_2 reaction and in the corresponding NO_2 calibration experiments, respectively. The factor γ is a correction accounting for the different degrees of absorption of the VUV probe laser radiation by the H_2S/O_2 mixture and NO_2, respectively. Absorption corrections were determined directly from the known distances inside the flow reactor and the relative difference in the VUV probe laser absorption measured in the reaction and calibration runs. Under typical experimental conditions absorption corrections were in the range $\gamma = 0.91-0.93$. With this calibration method a value of $\sigma_R(1.56\text{ eV}) = 0.22 \pm 0.05$ Å^2 was obtained. The experimental error was calculated from the errors of the entries of the calibration formula given above on the basis of simple error propagation. With the same calibration procedure a value of 0.24 ± 0.06 Å^2 was obtained for the translational energy of $E_{tr} = 1.66$ eV.

Discussion

The results of the present measurements are depicted in Figure 4 as filled circles along with the results of previous studies and compared with the results of the present quantum mechanical cross section calculations (solid line). As is obvious from Figure 4, the measurements based on O atom product detection (filled symbols in Figure 4) indicate a much less pronounced variation of the reaction cross section with translational energy than the earlier OH product state resolved measurements represented by the open symbols in Figure 4. In particular, the relatively sharp increase in reactivity in the energy range 1.2 eV $< E_{tr} <$ 1.7 eV is clearly absent in the O atom based measurements as well as in the accurate quantum mechanical calculations. The decrease of the reaction cross section at higher translational energies ($E_{tr} >$ 1.7 eV) which was also clearly observable in the recent O atom based measurements[40,41] has been tentatively attributed to the onset of nonadiabatic coupling to the electronically excited repulsive $HO_2(^2B_1)$ PES.[30] However, the latter hypothesis can only be properly tested in the framework of

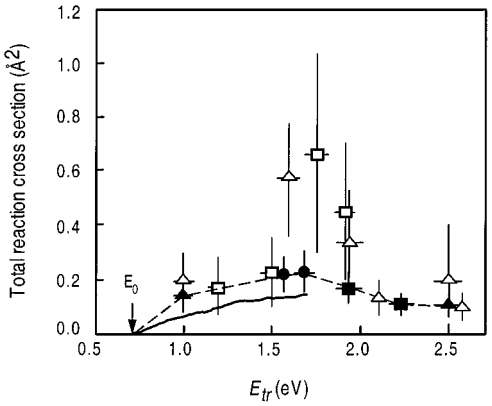

Figure 4. Total reaction cross sections for the $H + O_2(v = 0) \rightarrow OH + O$ reaction. The solid line describes the results of the present quantum scattering calculations. The open symbols □ and △ represent results of reaction cross sections measurements based on OH product detection as reported in refs 13 and 14, respectively. Filled symbols denote experimental reaction cross sections based on O atom detection; ● are the results of the present work, and ■ and ▲ denote reaction cross sections reported in refs 40 and 41, respectively. E_0 denotes the reaction threshold. Dashed lines are include to guide the eyes. For selected translational energies horizontal "error bars" are included to indicate the inherent spread of typically 0.15 eV (full-width half-maximum) of the corresponding experimental reagent translation energy distributions as typically present in gas-phase reaction dynamics studies of photolytically generated fast H atoms with room-temperature O_2 molecules.[38]

multisurface quantum scattering calculations on multiple PESs of HO_2.[32] An the other hand, comparison of the energy dependence of the present quantum mechanical cross sections obtained for translation energies below the C_{2v} conical intersection energy[30] with the revised experimental data suggests that the DMBE IV PES provides an reasonable representation of the $HO_2(\tilde{X}^2A'')$ ground-state potential. However, the fact that the absolute values of the calculated reaction cross sections are significantly lower than the experimental ones emphasizes the need for further improvements of this PES. This conclusion is in line with the results of most recent theoretical kinetics studies of the closely related $H + O_2 \rightarrow HO_2^*$ recombination reaction carried out by Troe and co-workers,[45,46] which revealed significant deficiencies of some of the previous ab initio data considered in the construction of the DMBE IV PES.

In summary, the agreement between experiment and quantum theory achieved in the present dynamics studies of the $H + O_2(v = 0) \rightarrow O + OH$ chain-branching reaction is encouraging and it can be expected that the consideration of the new ab initio information which was recently obtained[44] will soon results in an improved PES with a high enough accuracy to be used in quantum scattering calculations of thermal rate coefficients.

Acknowledgment. The present work was supported by the Deutsche Forschungsgemeinschaft via the Sonderforschungsbereich 359 "Reaktive Strömungen, Diffusion und Transport" at the University of Heidelberg and the National Science Foundation. We also acknowledge generous grants of computer time from the Argonne High Performance Computing Research Facility, the Maui High Performance Computing Center, and the National Partnership for Advanced Computer Infrastructure. T. Bohm, M. Cameron, A. Läuter, and H. P. Upadhyaya are thanked for their assistance during the course of the experimental investigations. The authors dedicate this article to Prof. Dr. Dres. h.c. Jürgen Troe on the occasion of his 60th birthday.

References and Notes

(1) Zare, R. N. *Science* **1998**, *279*, 1875.
(2) Clary, D. C. *Science* **1998**, *279*, 1879.
(3) Levine, R. D.; Bernstein, R. B. *Molecular Reaction Dynamics and Chemical Reactivity*; Oxford University Press: Oxford, U.K., 1987.
(4) Charutz, D. M.; Last, I.; Baer, M. *J. Chem. Phys.* **1997**, *106*, 7654.
(5) Wrede, E.; Schnieder, L.; Welge, K. H.; Aoiz, F. J.; Bañares, L.; Herrero, V. J. Martínez-Haya, B.; Sáez Rábanos, V. *J. Chem. Phys.* **1997**, *106*, 7862.
(6) Brownsword, R. A.; Hillenkamp, M.; Laurent, T.; Volpp, H.-R.; Wolfrum, J.; Vatsa, R. K.; Yoo, H.-S. *J. Phys. Chem.* **1997**, *101*, 6448.
(7) Jäckle, A.; Heitz, M.-C.; Meyer, H.-D. *J. Chem. Phys.* **1999**, *110*, 241.
(8) Miller, J. A.; Kee, R. J.; Westbrook, C. K. *Annu. Rev. Phys. Chem.* **1990**, *41*, 345.
(9) Troe, J. *Ber. Bunsen-Ges. Phys. Chem.* **1990**, *94*, 1183.
(10) Varandas, A. J. C. *Chem. Phys. Lett.* **1995**, *235*, 111 and references therein.
(11) To allow for comparison with previous experimental and theoretical results in the present report reaction cross sections are given in units of square-Ångstrøms, Å^2 (1 Å^2 = 10^{-20} m^2) and energies are given in units of eV (1 eV = 1.602 176 462 × 10^{-19} J).
(12) Kleinermanns, K.; Wolfrum, J. *J. Chem. Phys.* **1984**, *80*, 1446.
(13) Kessler, K.; Kleinermanns, K. *J. Chem. Phys.* **1992**, *97*, 374.
(14) Seeger, S.; Sick, V.; Volpp, H.-R.; Wolfrum, J. *Isr. J. Chem.* **1994**, *34*, 5.
(15) Miller, J. A.; Garrett, B. C. *Int. J. Chem. Kinet.* **1996**, *29*, 275.
(16) Bronikowski, M.; Zhang, R.; Rakestraw, D. J.; Zare, R. N. *Chem. Phys. Lett.* **1989**, *156*, 7.
(17) Fei, R.; Zheng, X. S.; Hall, G. E. *J. Phys. Chem. A* **1997**, *101*, 2541.
(18) In agreement with reaction dynamics experiments in which nascent OH($^2\Pi$) rotational fine-structure state population distributions were determined for different reagent translational energies the QCT calculations[10,15] indicated that depending on the reagent translational energy reaction 1 proceeds via two different reaction pathways.[16] At low energies ($E_0 < E_{tr} < 1.2$ eV), the reaction goes through a "floppy" activated HO_2^* reaction complex leading to statistical OH rotational distributions and differential cross sections which show a forward−backward symmetry as expected from long-lived collision complexes.[17] At higher energies, however, it was observed that the reaction follows a more direct pathway favoring the formation of highly rotational excited OH products[12−14] strongly forward scattered with respect to the initial H atom velocity direction.[17]
(19) Almi, R.; García-Vela, A.; Gerber, R. B. *J. Chem. Phys.* **1992**, *961*, 2034.
(20) Bowman, J. M.; Schatz, G. C. *Annu. Rev. Phys. Chem.* **1985**, *46*, 169 and references therein.
(21) Quack, M.; Troe, J. *Ber. Bunsen-Ges. Phys. Chem.* **1974**, *78*, 240.
(22) Troe, J. *J. Chem. Phys.* **1983**, *79*, 6017.
(23) Kuppermann, A.; Wu, Y.-M. *Chem. Phys. Lett.* **1993**, *205*, 599.
(24) de Miranda, M. P.; Clary, D. C.; Castillo, J. F.; Manolopoulos, D. E. *J. Chem. Phys.* **1998**, *108*, 3142.
(25) Manolopoulos, D. E. *J. Chem. Soc., Faraday Trans.* **1997**, *93* , 673.
(26) Zhang, D. H.; Zhang, J. Z. H. *J. Chem. Phys.* **1994**, *101*, 3671.
(27) Pack, R. T.; Butcher, E. A.; Parker, G. A. *J. Chem. Phys.* **1995**, *102*, 5998.
(28) Leforestier, C.; Miller, W. H. *J. Chem. Phys.* **1994**, *100*, 733.
(29) Pastrana, M. R.; Quintales, L. A. M.; Brandão, J.; Varandas, A. J. C. *J. Phys. Chem.* **1990**, *94*, 8073.
(30) Meijer, A. J. H. M.; Goldfield, E. M. *J. Chem. Phys.* **1999**, *110*, 870 and references therein.
(31) The combination of the symmetries of the H(^{2}S) and $O_2(^3\Sigma_g^-)$ reagents results in two PESs with ^{2}A″ and ^{4}A″ symmetry (in C_s point group), for which the lowest energy $HO_2(\tilde{X}^2A'')$ PES correlates adiabatically with OH($^2\Pi$) + O(^{3}P) products along a minimum energy path. However, for linear and T-shaped $H + O_2$ approach geometries barriers do exist resulting from the intersecting $^2\Sigma^-$ and $^2\Pi$ surfaces (in $C_{\infty v}$ point group) and the $^2A_2$ and $^2B_1$ surfaces (in C_{2v} point group), respectively.[31] The height of the adiabatic barrier due to the C_{2v} conical intersection has been calculated to be 1.7 eV with respect to the reagent zero-point energy. As a consequence, a rigorous treatment of the dynamics for $E_{tr} > 1.7$ eV would require multisurface scattering calculations on multiple PES of HO_2[32] that are outside the scope of the present theoretical study. Therefore, in the present work the translational energy range considered was restricted to energies below the C_{2v} conical intersection energy. Since we only take the single adiabatic $HO_2(\tilde{X}^2A'')$ PES into account in our calculations, we neglect the possible influence of Renner−Teller coupling between the $\tilde{X}^2A''$ and $1^2A'$ PES on the reaction probability. The latter PES correlates asymptotically to H(^{2}S) + $O_2(^1\Delta_g)$. The two PESs become degenerate at collinear reaction geometries at 0.5 eV above the asymptotic energy. However, the degeneracy lies in a direction perpendicular to the OH($^2\Pi$) + O(^{3}P) reaction coordinate,

making it less likely that this degeneracy will be important during the reaction. Thus, we still expect to obtain accurate results for the $H(^2S) + O_2(^3\Sigma_g^-) \rightarrow OH(^2\Pi) + O(^3P)$ reaction despite neglecting the coupling to the $1^2A'$ state in our calculations. A detailed discussion of the influence of the $1^2A'$ state on the temperature dependence of the thermal rate coefficient of the reverse reaction $OH(^2\Pi) + O(^3P)$ can be found in the paper by Troe.[9]

(32) Walch, S. P.; Rohlfing, C. M. *J. Chem. Phys*. **1989**, *91*, 2373.

(33) Kendrick, B.; Pack, R. T. *J. Chem. Phys.* **1995**, *102*, 1994.

(34) Press W. H.; Teukolsky, S. A.; Vetterling, W. T.; Flannery, B. P. *Numerical Recipes in Fortran: The Art of Scientific Computing*, 2nd ed.; Cambridge University Press: New York, 1992; p 644.

(35) For the homonuclear diatomic molecule $^{16}O_2$ in its electronic ground state ($X^3\Sigma_g^-$) only odd-numbered rotational states are allowed by symmetry.

(36) Varandas, A. J. C. *Mol. Phys.* **1995**, *85*, 1159.

(37) Meijer, A. J. H. M.; Goldfield, E. M. *Phys. Chem. Chem. Phys.*, submitted.

(38) Goldfield, E. M.; Meijer, A. J. H. M. *J. Chem. Phys.* **2000**, *113*, 11055.

(39) Kuppermann, A. *Isr. J. Chem.* **1969**, *7*, 303.

(40) van der Zande, W. J.; Zhang, R.; Zare, R. N.; McKendrick, K. G.; Valentini, J. J. *J. Phys. Chem.* **1991**, *95*, 5, 8205.

(41) Rubahn, H.-G.; van der Zande, W. J.; Zhang, R.; Bronikowski, M. J.; Zare, R. N. *Chem. Phys. Lett.* **1991**, *186*, 154.

(42) Ebert, V.; Schulz, C.; Volpp, H.-R.; Wolfrum, J.; Monkhouse, P. *Isr. J. Chem.* **1999,** *39*, 1.

(43) Schulz, C.; Volpp, H.-R.; Wolfrum, J. In *Chemical Dynamics in Extreme Environments*; Dressler, R., Ed.; World Scientific: Singapore, in press.

(44) The previous reaction cross section measurements reported in refs 12−14 were based on spin−orbit fine structure and Λ-doublet rotational state resolved $OH(^2\Pi)$ product detection by laser-induced fluorescence (LIF) excitation employing the diagonal bands of the $OH(^2\Sigma^+ \leftarrow {}^2\Pi)$ transition in the 306−323 nm ultraviolet spectral region. However, due to predissociation of the electronically excited state $^2\Sigma^+$ state of OH with this LIF detection scheme only those $OH(^2\Pi)$ product radicals formed in the vibrational ground state and in the first vibrational excited state can be detected. As a consequence, in the reaction cross section measurements at higher collision energies where significant amounts of $OH(v > 1)$ can be produced, the contribution of the higher OH product vibrational states to the total reactive cross section had to be estimated by extrapolation.

(45) Troe, J. *28th Symposium (International) on Combustion*; The Combustion Institute: Pittsburgh, PA, in press.

(46) Harding, L. B.; Troe, J.; Ushakov, V. G. *Phys. Chem. Chem. Phys.* **2000**, *2*, 631.